Correlation functions in an ionic liquid at coexistence with an ionic crystal: results of the Brazovskii-type field theory

2007 J. Phys.: Condens. Matter 19 236203

(http://iopscience.iop.org/0953-8984/19/23/236203)

IOP PUBLISHING JOURNAL OF PHYSICS: CONDENSED MATTER

J. Phys.: Condens. Matter **19** (2007) 236203 (20pp) doi:10.1088/0953-8984/19/23/236203

Correlation functions in an ionic liquid at coexistence with an ionic crystal: results of the Brazovskii-type field theory

O Patsahan[1] **and A Ciach**[2]

[1] Institute for Condensed Matter Physics of the National Academy of Sciences of Ukraine, 79011 Lviv, Ukraine
[2] Institute of Physical Chemistry, Polish Academy of Sciences, 01-224 Warszawa, Poland

E-mail: oksana@icmp.lviv.ua

Received 7 September 2006, in final form 16 April 2007
Published 8 May 2007
Online at stacks.iop.org/JPhysCM/19/236203

Abstract

Correlation functions in the restricted primitive model are calculated within a field-theoretic approach in the one-loop self-consistent Hartree approximation. The correlation functions exhibit damped oscillatory behaviour as found before in the Gaussian approximation (Ciach *et al* 2003 *J. Chem. Phys.* **118** 3702). The fluctuation contribution leads to a renormalization of both the amplitude and the decay length of the correlation functions. The renormalized quantities show qualitatively different behaviour than their mean-field (MF) counterparts. While the amplitude and the decay length both diverge in the MF when the λ-line is approached, the renormalized quantities remain of order of unity in the same dimensionless units down to the coexistence with the ionic crystal. Along the line of the phase transition the decay length and the period of oscillations are independent of density, and their values in units of the diameter of the ions are $\alpha_0^{-1} \approx 1$ and $2\pi/\alpha_1 \approx 2.8$ respectively.

Dedicated to Professor R Evans on the occasion of his 60th birthday.

1. Introduction

The distribution of charges in ionic systems has been a subject of considerable interest for many years. In theoretical studies of systems such as molten salts, electrolytes or ionic liquids the interaction potential is often approximated by the restricted primitive model (RPM), where identical hard spheres carry positive or negative charges with equal magnitude. Earlier studies concentrated on correlation functions for charges in ion-dilute systems [1–3], and later the ion-dense systems were also investigated [2–9]. However, the question of the form of the correlation functions in a liquid (fused salt) at coexistence with an ionic crystal remains open. The correlation functions in a liquid phase can be quite accurately described within liquid

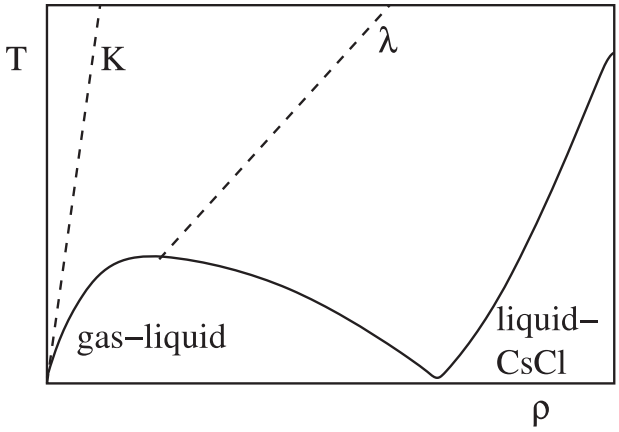

Figure 1. A portion of the density–temperature phase diagram for the RPM as obtained in MF, shown schematically. Solid lines separate the uniform fluid from the two-phase regions. Dashed lines denoted by K and λ represent the Kirkwood line and the λ-line respectively. T and ρ are in arbitrary units.

theories such as the mean-spherical approximation (MSA) [3, 5]. However, the transition to a crystalline phase is not predicted by the liquid theories. The liquid–solid transition in the RPM was determined within the density functional theory of freezing in [10], but the charge–charge correlation function was not discussed in this work. Both the phase transition and the correlation functions can be found on the same level of approximation within the framework of the field theory introduced for the RPM in [11]. Phase coexistence with an ionic crystal was recently found within the field-theoretic framework in [12] by applying the Brazovskii-type approximation. The correlation functions are calculated in the same approximation in this work. We pay particular attention to the decay length, the period of damped oscillations and the amplitude along the phase coexistence with an ionic crystal.

Let us summarize the results of earlier theories. The behaviour of the charge–charge correlation function $h_{\mathrm{D}}(x)$ depends on thermodynamic conditions. In figure 1 a portion of the density–temperature phase diagram, as obtained in different theoretical [2, 3] and simulation [13] studies, is shown schematically. Usually the density and temperature are given in the standard reduced units, $\rho^* = \rho\sigma^3$ and $T^* = k_{\mathrm{B}}T\frac{D\sigma}{e^2}$ respectively, where σ, e, D, k_{B} and T are the diameter and the charge of the ion, the dielectric constant, the Boltzmann constant and temperature respectively. It is convenient to introduce the parameter

$$S \equiv \frac{T^*}{\rho^*} = \frac{4\pi}{x_{\mathrm{D}}^2}, \tag{1}$$

where

$$x_{\mathrm{D}} = \kappa_{\mathrm{D}}\sigma = \sqrt{4\pi\beta^*\rho^*} \tag{2}$$

is the dimensionless inverse Debye length, and $\beta^* = 1/T^*$. The solid lines in figure 1 represent boundaries of stability of the uniform fluid phase, and regions corresponding to different qualitative properties of $h_{\mathrm{D}}(x)$ are separated by the dashed lines. The Kirkwood line (K) $S = S_{\mathrm{K}}$ separates the high-temperature/low-density region $S > S_{\mathrm{K}}$, corresponding to an asymptotic monotonic decay of correlations,

$$xh_{\mathrm{D}}(x)\rho^{*2} = A^{(1)}\mathrm{e}^{-a_1 x} + A^{(2)}\mathrm{e}^{-a_2 x}, \tag{3}$$

from the low-temperature/high-density region $S < S_K$, corresponding to exponentially damped oscillatory behaviour of $h_D(x)$,

$$xh_D(x)\rho^{*2} = -\mathcal{A}_{\phi\phi}\sin(\alpha_1 x + \theta)e^{-\alpha_0 x}. \tag{4}$$

In MF theories [5, 14, 15] the Kirkwood line is a straight line, and its slope was found to be $S_K \approx 8.33$ in the GMSA [5], with similar results in other liquid theories, and $S_K \approx 11.8$ [15] on the MF level of the field theory [11].

For $S \to S_K^+$ the two dominant imaginary poles of $\tilde{h}_D(k)$, ia_1 and ia_2, merge together, and for $S < S_K$ a pair of conjugate complex poles, $i\alpha_0 \pm \alpha_1$, appears. The remaining poles modify the short-distance behaviour (up to $\sim 3\sigma$ [5]). There is no controversy concerning this line, but there are no general reasons for this line to be straight beyond MF [3].

When the λ-line $S = S_\lambda$ is approached from the high-temperature side, the conjugate complex poles of $\tilde{h}_D(k)$ reach the real axis. Both the decay length α_0^{-1} and the amplitude $\mathcal{A}_{\phi\phi}$ of the correlation function diverge as $(S - S_\lambda)^{-1/2}$, [11, 14–16]. The low-temperature side of this line corresponds to a charge-ordered structure, where the nearest neighbours (nns) are oppositely charged. The λ-line represents a continuous transition between the uniform and the charge-ordered phases at temperatures higher than the tricritical-point temperature. At temperatures lower than the tricritical-point temperature the λ-line represents a spinodal. The slope of this line, S_λ, shows a strong dependence on approximations and assumptions made in different theories [14]. In particular, in the MF approximation for the field theory $S_\lambda \approx 1.6$ was obtained [11], whereas the MSA yields $S_\lambda = 0$ [5]. The charge-ordered liquid phase has not been observed either experimentally or in simulations. A natural conclusion would be to question the validity of theories that predict the existence of the λ-line. However, the λ-line of continuous transitions to the charge-ordered phase was observed in simulations [17–19] in the lattice version of the RPM (LRPM), in agreement with predictions of the lattice version of the field theory [20]. Some other theories [21–23] yield similar results for the LRPM. The MSA, however, predicts an absence of such a transition in the LRPM. One might argue that the MSA theories are correct only in the continuum space, and the field theory yields correct results only on the lattice. This is indeed the case for the field theory in the MF approximation. However, fluctuations play a very important role in the RPM. Beyond MF, with the charge fluctuations accounted for in a Brazovskii-type approximation [12, 24, 25], the decay length of the charge–charge correlation function does not diverge in the continuum-space RPM [12], but its value has not been found yet. At the same time a first-order transition to an ionic crystal is found [12] for the range of densities and temperatures that agrees with simulations [13].

The field-theory results [12, 24, 25] shed light on the nature of the λ-line in continuum space; it separates the stability region of the disordered phase on the phase diagram (ρ^*, T^*) into two regions that correspond to different forms of the *most probable* instantaneous distributions of ions. At the high-temperature side of the line $S = S_\lambda$ the distribution of ions is most probably random. For $S < S_\lambda$, however, the most probable instantaneous distributions of the ions correspond to charge-density waves with the wavelength $\sim 2.5\sigma$. According to the above prediction, in real-space representation charge-ordered clusters with an nn distance $\sim 1.27\sigma$ should dominate over randomly distributed ions in microscopic states of the disordered phase. Such structures were indeed seen in simulation snapshots [26–28]. Our purpose is to verify if the instantaneous order has some effect on the correlation functions beyond the MF approximation.

In [15] the correlation functions were calculated in the MF (Gaussian) approximation within the framework of the field-theoretic description developed in [11]. In this work we consider a simple criterion of validity of the MF (Gaussian) approximation for a system where the dominant fluctuations of the order parameter are periodic in space. The criterion

is formulated in terms of the MF correlation functions. An important feature is a strong dependence of the validity of the MF approximation for $\tilde{h}_{\rm D}(k)$ on k. We present a derivation of the criterion, which is next used for a verification of the validity of the MF in the RPM. The results of [15] are extended beyond the Gaussian approximation, and the correlation functions are calculated to a one-loop order. In the phase-space region where the MF is qualitatively wrong, the self-consistent one-loop approximation is used, as in the Brazovskii theory [29]. We verify that the Brazovskii theory is valid, at least semiquantitatively, near the coexistence with the ionic crystal. Liquid–crystal coexistence was obtained earlier in [12]. We find that the amplitude and the decay length are quite small at the coexistence. This result shows that the pair-correlation functions cannot give any information on the process of clustering of ions observed in individual microstates.

In the next section we briefly present the field-theoretic description of the RPM. Definitions of the quantities relevant for the present work are given, and notation is fixed in section 2.1. Section 2.2 is devoted to a short summary of earlier results obtained in the MF approximation. In section 2.3 we briefly describe the weighted-field approximation [11, 30] that is used in our calculations. Sections 3 and 4 contain results obtained in the present work. A criterion of the validity of the MF approximation for the structure factor is derived and applied to the RPM in section 3. In section 4 the correlation functions are calculated in the Brazovskii theory [29].

2. Background

2.1. Field-theoretic description of the RPM

In the field theory derived for the RPM in [11, 25, 30] the fluctuating order-parameter (OP) fields are the local deviations from the most probable number and charge densities, $\eta(\mathbf{x}) = \rho^*(\mathbf{x}) - \rho_0^*(\mathbf{x})$ and $\Delta\phi(\mathbf{x}) = \phi(\mathbf{x}) - \phi_0(\mathbf{x})$ respectively, where $\rho(\mathbf{x}) = \rho_+^*(\mathbf{x}) + \rho_-^*(\mathbf{x})$ and $\phi(\mathbf{x}) = \rho_+^*(\mathbf{x}) - \rho_-^*(\mathbf{x})$, with analogous definitions for the most probable quantities for which the subscript 0 is used. The subscripts $+$ and $-$ refer to cations and anions, respectively. Asterisks indicate that all densities are dimensionless (the unit volume is σ^3). $e\phi$ is the charge density in e/σ^3 units. We focus on systems that are globally charge-neutral,

$$\int_{\mathbf{x}} \phi(\mathbf{x}) = 0, \tag{5}$$

where in this paper we use the notation $\int_{\mathbf{x}} \equiv \int \mathrm{d}\mathbf{x}$. The fields $\eta(\mathbf{x})$ and $\Delta\phi(\mathbf{x})$ are thermally excited with the probability density [11, 25, 31]

$$p[\phi, \eta] = \Xi^{-1} \exp(-\beta \Delta\Omega^{\rm MF}[\phi, \eta]), \tag{6}$$

where β is the reciprocal temperature ($\beta = 1/k_{\rm B}T$),

$$\Xi = \int D\phi D\eta \exp(-\beta \Delta\Omega^{\rm MF}[\phi, \eta]) \tag{7}$$

is the normalization constant, and

$$\Delta\Omega^{\rm MF}[\phi, \eta] = \Omega^{\rm MF}[\phi(\mathbf{x}), \rho^*(\mathbf{x})] - \Omega^{\rm MF}[\phi_0(\mathbf{x}), \rho_0^*(\mathbf{x})], \tag{8}$$

where for $\phi(\mathbf{x}) = \phi_0(\mathbf{x})$ and $\rho^*(\mathbf{x}) = \rho_0^*(\mathbf{x})$ the $\Omega^{\rm MF}[\phi, \rho^*]$ assumes a minimum. $\Omega^{\rm MF}[\phi, \rho^*]$ is the grand-thermodynamic potential in a system where the OP fields are constrained to have the given forms $\phi(\mathbf{x})$ and $\rho^*(\mathbf{x})$.

In the theory studied in [11, 15, 25] the explicit expression for $\Omega^{\rm MF}[\phi, \rho^*]$ is given by

$$\Omega^{\rm MF}[\phi, \rho^*] = F_{\rm h}[\phi, \rho^*] + U[\phi] - \mu \int_{\mathbf{x}} \rho(\mathbf{x}). \tag{9}$$

In the above, μ is the chemical potential of the ions (for the RPM, $\mu_+ = \mu_- = \mu$), $F_{\rm h}[\phi, \rho^*] = \int_{\mathbf{x}} f_{\rm h}(\phi(\mathbf{x}), \rho^*(\mathbf{x}))$ is the hard-core reference-system Helmholtz free energy of the mixture in which the core-diameter σ of both components is the same. We use the Carnahan–Starling (CS) form of $f_{\rm h}(\phi, \rho^*)$ in the local-density approximation, as in [12]. Finally, the energy in the RPM is given by

$$\beta U[\phi] = \frac{\beta^*}{2} \int_{\mathbf{x}} \int_{\mathbf{x}'} \frac{\theta(|\mathbf{x}' - \mathbf{x}| - 1)}{|\mathbf{x} - \mathbf{x}'|} \phi(\mathbf{x})\phi(\mathbf{x}') = \frac{\beta^*}{2} \int_{\mathbf{k}} \tilde{\phi}(\mathbf{k})\tilde{V}(k)\tilde{\phi}(-\mathbf{k}), \quad (10)$$

where $\int_{\mathbf{k}} \equiv \int d\mathbf{k}/(2\pi)^3$, and $\tilde{f}(\mathbf{k})$ denotes a Fourier transform of $f(\mathbf{x})$. Contributions to the electrostatic energy coming from overlapping cores are not included in (10). Here and below the distance is measured in σ units. The Fourier transform of the dimensionless Coulomb potential $V(x) = \theta(x - 1)/x$, where $x = |\mathbf{x}|$, is

$$\tilde{V}(k) = 4\pi \cos k/k^2, \quad (11)$$

where k is in σ^{-1} units.

In the system with no constraint on the form of the OP fields, which can fluctuate about the most probable values with the probability (6), the grand-thermodynamic potential is given by the standard statistical–mechanical relation

$$\Omega = \Omega^{\rm MF}[\phi_0(\mathbf{x}), \rho_0^*(\mathbf{x})] - k_{\rm B}T \log \Xi, \quad (12)$$

where the second term is the contribution to Ω associated with fluctuations about the most probable fields $\phi_0(\mathbf{x})$, $\rho_0^*(\mathbf{x})$. In this work we limit ourselves to the disordered phase, where $\phi_0(\mathbf{x}) = 0$, and hence $\Delta\phi = \phi$, and $\rho_0^*(\mathbf{x}) = \rho_0^* =$ constant. The correlation function for the fields $f = \phi, \eta$, and $g = \phi, \eta$ is defined by

$$G_{fg}(\Delta x) = \langle f(\mathbf{x}_1)g(\mathbf{x}_2)\rangle^{\rm con} \quad (13)$$

where $\Delta x = |\mathbf{x}_1 - \mathbf{x}_2|$, and

$$\langle f(\mathbf{x}_1)g(\mathbf{x}_2)\rangle^{\rm con} \equiv \langle f(\mathbf{x}_1)g(\mathbf{x}_2)\rangle - \langle f(\mathbf{x}_1)\rangle\langle g(\mathbf{x}_2)\rangle, \quad (14)$$

and $\langle A[\phi, \eta]\rangle$ denotes the average value of the quantity $A[\phi, \eta]$, with the probability given by the Boltzmann factor (6). The charge-density correlation function $G_{\phi\phi}$ is related to the analogue of the total charge–charge correlation function $h_{\rm D}(x)$ [3, 5], and in Fourier representation this relation is given by

$$\frac{\tilde{G}_{\phi\phi}(k)}{\langle\rho^*\rangle} = \tilde{h}_{\rm D}(k)\langle\rho^*\rangle + 1. \quad (15)$$

2.2. Mean-field approximation

In the mean-field (MF) approximation, equivalent to the random phase approximation (RPA), Ω (equation (12)) in the fluid phase is just approximated by $\Omega^{\rm MF}[0, \rho_0^*]$. In the ordered phase Ω is approximated by another minimum of $\Omega^{\rm MF}[\phi, \rho^*]$, corresponding to $\phi_0(\mathbf{x})$ and $\rho_0(\mathbf{x})$ that are periodic in space. Here we limit ourselves to the disordered phase. The functional $\Delta\Omega^{\rm MF}[\phi, \eta]$ (equations (8) and (9)) can be separated into two parts,

$$\Delta\Omega^{\rm MF}[\phi, \eta] = \Omega_2[\phi, \eta] + \Omega_{\rm int}[\phi, \eta], \quad (16)$$

where the Gaussian part is

$$\beta\Omega_2[\phi, \eta] = \tfrac{1}{2} \int_{\mathbf{k}} \tilde{\phi}(\mathbf{k})\tilde{C}^0_{\phi\phi}(k)\tilde{\phi}(-\mathbf{k}) + \tfrac{1}{2} \int_{\mathbf{k}} \tilde{\eta}(\mathbf{k})\tilde{C}^0_{\eta\eta}(k)\tilde{\eta}(-\mathbf{k}), \quad (17)$$

with

$$\tilde{C}^0_{ff}(k) = \left.\frac{\delta\beta\Delta\Omega^{\rm MF}}{\delta\tilde{f}(\mathbf{k})\delta\tilde{f}(-\mathbf{k})}\right|_{f=0}. \tag{18}$$

The MF approximation for G_{ff} is denoted by G^0_{ff}, and is identified with the Gaussian approximation. In the Gaussian approximation the correlation functions are given in equation (14), with the approximation $\Delta\Omega^{\rm MF} = \Omega_2$ used in the Boltzmann factor (6) ($\Omega_{\rm int}[\phi, \eta]$ is neglected in equation (16)). Since the two OP fields are decoupled in Ω_2, in Fourier representation

$$\tilde{G}^0_{ff}(k) = 1/\tilde{C}^0_{ff}(k),$$

as can be verified easily.

The charge-density correlation function in the MF approximation was studied in [15]. In Fourier representation $\tilde{G}^0_{\phi\phi}(k)$ is given by

$$\tilde{G}^0_{\phi\phi}(k) = \tilde{C}^{0-1}_{\phi\phi}(k) = \frac{T^*}{\left(S + \tilde{V}(k)\right)} = \frac{T^*}{(S - S_\lambda + \Delta\tilde{V}(k))}, \tag{19}$$

where S is defined in equation (1),

$$S_\lambda \equiv -\tilde{V}(k_b) \approx 1.61, \tag{20}$$

$$\Delta\tilde{V}(k) = \tilde{V}(k) - \tilde{V}(k_b) \simeq_{k\to k_b} v_2(k - k_b)^2 + {\rm O}((k - k_b)^3), \tag{21}$$

$v_2 \approx 1.07$, and $k_b \approx 2.46$ corresponds to the minimum, $\tilde{V}(k_b) \approx -1.61$, of $\tilde{V}(k)$ given in equation (11).

Let us first focus on the behaviour of $\tilde{G}^0_{\phi\phi}(k)$ for $k \to 0$. From (19) and (11) we obtain

$$\frac{\tilde{G}^0_{\phi\phi}(k)}{\rho_0^*} \simeq_{k\to 0} \frac{Sk^2}{(S - 2\pi)k^2 + 4\pi} \simeq_{k\to 0} \frac{S}{4\pi}k^2. \tag{22}$$

For $S \to \infty$ the first relation in (22) reduces to the form

$$\frac{\tilde{G}^0_{\phi\phi}(k)}{\rho_0^*} \simeq_{k\to 0} \frac{k^2}{k^2 + x_{\rm D}^2}, \tag{23}$$

where the dimensionless inverse Debye length $x_{\rm D}$ is given in (2). Note that equation (23) (with equation (15)) is consistent with the exact second-moment condition of Stillinger and Lovett [3, 4] as well as with the Debye–Hückel result.

For $k \neq 0$ the properties of $\tilde{G}^0_{\phi\phi}(k)$ agree with the results of other theories [14] only qualitatively [15]. The qualitative agreement with the GMSA results for $\tilde{h}_{\rm D}(k)$ [5] is found only in the phase-space region given by $S \gg S_\lambda$, where S and S_λ are defined in equations (1) and (20). The λ-line, $S = S_\lambda$, represents the boundary of stability of the functional $\Delta\Omega^{\rm MF}$ in the (ρ_0^*, T^*) phase diagram [12, 25], because at this line the second functional-derivative of $\Delta\Omega^{\rm MF}$ vanishes for $k = k_b$, where k_b is the wavenumber of the most probable fluctuations $\tilde{\phi}(\mathbf{k}_b)$ [25, 32] (see (19)). No such instability is found in the GMSA, as discussed already in the introduction.

The charge-density correlation function in real-space representation is obtained in [15] by a pole analysis of $\tilde{G}^0_{\phi\phi}(k)$ (equation (19)). The behaviour described in the introduction was obtained with $S = S_{\rm K} \approx 11.8$. The explicit expressions for the amplitude $\mathcal{A}_{\phi\phi}$, the phase θ and the inverse lengths α_0 and α_1 are given in [15]. When the λ-line is approached, both α_0^{-1} and $\mathcal{A}_{\phi\phi}$ diverge as $\propto (S - S_\lambda)^{-1/2}$, whereas $\theta \propto (S - S_\lambda)^{1/2}$ and $\alpha_1 \to k_b$.

The number-density correlation function in the above MF theory for the RPM has the trivial form

$$G^0_{\eta\eta}(\mathbf{x}-\mathbf{x}') = G^0_{\eta\eta}\delta(\mathbf{x}-\mathbf{x}'), \qquad \text{where } G^0_{\eta\eta} = \left[\frac{\partial^2 f_{\rm h}}{\partial\rho^{*2}}\right]^{-1}, \tag{24}$$

because the microscopic structure associated with hard spheres is suppressed in the coarse-grained description.

Beyond MF the second term in equation (12) is included. This term represents the fluctuation contribution to the grand potential. In [12] the Brazovskii theory [29] is chosen to find the approximate form of this term in the disordered and the ordered phases. In this work the same approximation is chosen for a determination of the correlation functions.

2.3. Weighted-field approximation

The two OP fields are not equivalent, because in the RPM only charges interact. For this reason it is possible to simplify the field theory [25, 33]. In this work we focus on the weighted-field (WF) approximation introduced in [11], and described in more detail in [25, 30, 31]. In the WF approximation the field $\eta(\mathbf{x})$ is approximated by its most probable form for each given field $\phi(\mathbf{x})$. For the given field $\phi(\mathbf{x})$ the most probable field η corresponds to the minimum of $\beta\Delta\Omega^{\rm MF}[\phi,\eta]$ and is determined by $\delta\Delta\Omega^{\rm MF}/\delta\eta = 0$. Thus, in the WF approximation the field $\eta(\mathbf{x})$ assumes the form

$$\eta_{\rm WF}(\phi(\mathbf{x})) = \sum_n \frac{a_n}{n!}\phi(\mathbf{x})^{2n}, \tag{25}$$

where a_n are functions of ρ^*_0 [12, 30]. The Boltzmann factor (6) and Ξ in the WF reduce to the forms

$$p_{\rm WF}[\phi] = \Xi^{-1}_{\rm WF}{\rm e}^{-\beta\mathcal{H}_{\rm WF}[\phi]}. \tag{26}$$

$$\Xi_{\rm WF} = \int D\phi{\rm e}^{-\beta\mathcal{H}_{\rm WF}[\phi]}, \tag{27}$$

where $\mathcal{H}_{\rm WF}[\phi] = \Delta\Omega^{\rm MF}[\phi,\eta_{\rm WF}[\phi]]$.

We truncate the expansion in (25) at $n = 2$, and limit ourselves to the ϕ^6 theory, with $\mathcal{H}_{\rm WF}$ approximated by

$$\beta\mathcal{H}_{\rm WF}[\phi] = \frac{1}{2}\int_{\mathbf{x}}\int_{\mathbf{x}'}\phi(\mathbf{x})C^0_{\phi\phi}(\mathbf{x}-\mathbf{x}')\phi(\mathbf{x}') + \frac{\mathcal{A}_4}{4!}\int_{\mathbf{x}}\phi^4(\mathbf{x}) + \frac{\mathcal{A}_6}{6!}\int_{\mathbf{x}}\phi^6(\mathbf{x}) + {\rm O}(\phi^8), \tag{28}$$

The explicit forms of $\mathcal{A}_4(\rho^*_0)$ and $\mathcal{A}_6(\rho^*_0)$ were found in [12], and for the convenience of the reader are given in appendix A. In this work we consider only $\rho^*_0 > 0.1541$; for this range of densities $\mathcal{A}_6(\rho^*_0) > 0$. For $\mathcal{A}_6(\rho^*_0) < 0$ the term ${\rm O}(\phi^8)$ must be included for stability reasons. One should remember that the accuracy of the results obtained with the above functional depends on how large the neglected contributions to $\beta\mathcal{H}_{\rm WF}[\phi]$ are.

In the above ϕ^6 theory the charge-density correlation function is given in equation (13) with the probability distribution approximated by equation (26). In the following $\langle\cdots\rangle$ denotes the average in the WF approximation. The average density in the disordered phase and the number-density correlation function for $\mathbf{x} \neq \mathbf{x}'$ are approximated by [12, 15]

$$\langle\rho^*(\mathbf{x})\rangle = \rho^*_0 + a_1\langle\phi(\mathbf{x})^2\rangle + \frac{a_2}{2!}\langle\phi(\mathbf{x})^4\rangle, \tag{29}$$

and

$$\begin{aligned} G_{\eta\eta}(\mathbf{x},\mathbf{x}') \equiv{}& G^0_{\eta\eta}\delta(\mathbf{x},\mathbf{x}') + \langle\eta_{\rm WF}(\mathbf{x})\eta_{\rm WF}(\mathbf{x}')\rangle^{\rm con} = G^0_{\eta\eta}\delta(\mathbf{x},\mathbf{x}') \\ &+ a_1^2\langle\phi^2(\mathbf{x})\phi^2(\mathbf{x}')\rangle^{\rm con} + \frac{a_1a_2}{2}(\langle\phi^4(\mathbf{x})\phi^2(\mathbf{x}')\rangle^{\rm con} + (\mathbf{x}\leftrightarrow\mathbf{x}')) \\ &+ \frac{a_2^2}{4}\langle\phi^4(\mathbf{x})\phi^4(\mathbf{x}')\rangle^{\rm con}, \end{aligned} \tag{30}$$

where the explicit forms of $a_1(\rho_0^*)$ and $a_2(\rho_0^*)$, obtained in [12], are given in appendix A. We should stress that beyond the local-density approximation for $F_{\rm h}$ in equation (9), the first term in (30) should be replaced by the non-local hard-sphere contribution.

3. Verification of validity of the MF approximation

We first present main steps of a derivation of the criterion of validity of the MF approximation for the correlation function. Let us rewrite (28) in the form

$$\mathcal{H}_{\rm WF}[\phi] = \mathcal{H}_0[\phi] + \mathcal{H}_{\rm int}[\phi], \tag{31}$$

where

$$\mathcal{H}_0[\phi] = \tfrac{1}{2}\int_{\mathbf{x}}\int_{\mathbf{x}'} \phi(\mathbf{x})C^0_{\phi\phi}(\mathbf{x}-\mathbf{x}')\phi(\mathbf{x}'). \tag{32}$$

In order to verify the validity of the MF approximation for the charge-density correlation function, $G_{\phi\phi}$, we calculate the lowest-order correction and compare it with $G^0_{\phi\phi}$. The MF is valid when the correction term is negligible compared to $G^0_{\phi\phi}$. The correction term is present when $\mathcal{H}_{\rm int}$ is included in equation (31). Let us assume that $\mathcal{H}_{\rm int} \ll \mathcal{H}_0$, and $\exp(-\beta\mathcal{H}_{\rm WF})$ can be expanded about $\exp(-\beta\mathcal{H}_0)$ in (27). We truncate the expansion at the first-order term, and in this approximation we obtain

$$\Xi_{\rm WF} = \Xi_0\left[1 - \frac{\mathcal{A}_4}{4!}\int_{\mathbf{x}}\langle\phi^4(\mathbf{x})\rangle_0 + {\rm O}(\mathcal{A}_4^2, \mathcal{A}_6)\right], \tag{33}$$

where

$$\Xi_0 = \int D\phi {\rm e}^{-\beta\mathcal{H}_0} \tag{34}$$

and $\langle\cdots\rangle_0$ denotes averaging with the Gaussian probability $p = \Xi_0^{-1}\exp(-\beta\mathcal{H}_0)$. At the same order of approximation (with terms ${\rm O}(\mathcal{A}_4^2, \mathcal{A}_6)$ neglected) we have

$$\langle\phi(\mathbf{x}_1)\phi(\mathbf{x}_2)\rangle\,\Xi_{\rm WF} = \int D\phi {\rm e}^{-\beta\mathcal{H}_0}\phi(\mathbf{x}_1)\phi(\mathbf{x}_2) - \frac{\mathcal{A}_4}{4!}\int D\phi {\rm e}^{-\beta\mathcal{H}_0}\phi(\mathbf{x}_1)\phi(\mathbf{x}_2)\int_{\mathbf{x}}\phi^4(\mathbf{x}). \tag{35}$$

From (33) and (35) we obtain

$$\begin{aligned}\langle\phi(\mathbf{x}_1)\phi(\mathbf{x}_2)\rangle = {}& \langle\phi(\mathbf{x}_1)\phi(\mathbf{x}_2)\rangle_0 + \frac{\mathcal{A}_4}{4!}\int_{\mathbf{x}}\langle\phi(\mathbf{x}_1)\phi(\mathbf{x}_2)\rangle_0\langle\phi^4(\mathbf{x})\rangle_0 \\ & - \frac{\mathcal{A}_4}{4!}\int_{\mathbf{x}}\langle\phi(\mathbf{x}_1)\phi(\mathbf{x}_2)\phi^4(\mathbf{x})\rangle_0 + {\rm O}(\mathcal{A}_4^2, \mathcal{A}_6).\end{aligned} \tag{36}$$

In Fourier representation the above takes the form

$$\tilde{G}_{\phi\phi}(k) = \tilde{G}^0_{\phi\phi}(k)\left(1 - \frac{\mathcal{A}_4}{2}\mathcal{G}_0\tilde{G}^0_{\phi\phi}(k) + {\rm O}(\mathcal{A}_4^2, \mathcal{A}_6)\right), \tag{37}$$

where

$$\mathcal{G}_0 = \int_{\mathbf{k}}\tilde{G}^0_{\phi\phi}(k). \tag{38}$$

Terms ${\rm O}(\mathcal{A}_4^2, \mathcal{A}_6)$ in equation (37) appear when the perturbation expansion of $\exp(-\beta\mathcal{H}_{\rm WF})$ about $\exp(-\beta\mathcal{H}_0)$ is truncated at a higher-order term, and can be obtained in a similar way. Each term in the perturbation expansion can be conveniently represented by a Feynman diagram, where a line connecting points $\mathbf{x}$ and $\mathbf{x}'$ represents $G^0_{\phi\phi}(\mathbf{x}-\mathbf{x}')$, and $-\mathcal{A}_4$ or $-\mathcal{A}_6$ represent vertices from which 4 or 6 lines emanate. Finally, a space integration is associated with each vertex, or in Fourier representation an integration is associated with each

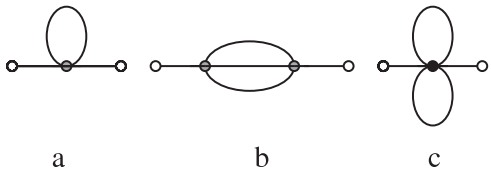

Figure 2. Feynman diagrams contributing to $G_{\phi\phi}$ to two-loop order. The shaded circle and the bullet represent $-\mathcal{A}_4$ and $-\mathcal{A}_6$ respectively, and external points are represented by open circles. Lines connecting points $\mathbf{x}_1$ and $\mathbf{x}_2$ represent $G^0_{\phi\phi}(\mathbf{x}_1 - \mathbf{x}_2)$.

loop. Numerical factors in the perturbation expansion are associated with a symmetry of the corresponding graph. In figure 2 the Feynman diagrams contributing to $G_{\phi\phi}$ are shown up to two-loop order. The lowest-order correction to $G^0_{\phi\phi}(\mathbf{x} - \mathbf{x}')$ (see (37)) is represented by the diagram shown in figure 2(a).

The MF approximation is correct when

$$\tilde{b}(k) = \frac{\mathcal{A}_4}{2}\mathcal{G}_0\tilde{G}^0_{\phi\phi}(k) \ll 1. \tag{39}$$

Note that the lowest-order correction to $\tilde{G}_{\phi\phi}(k)$ depends strongly on k (through $\tilde{G}^0_{\phi\phi}(k)$), and also on the whole spectrum of the wavelengths (through $\mathcal{G}_0$).

Let us first analyse the properties of $\mathcal{G}_0$, explicitly given by

$$\mathcal{G}_0 = \frac{T^*}{2\pi^2}\int_0^\infty \mathrm{d}k\, f(k) \tag{40}$$

where

$$f(k) = k^2\tilde{G}^0_{\phi\phi}(k) = \frac{k^4}{Sk^2 + 4\pi\cos(k)}. \tag{41}$$

The integral (40) diverges because for $k \to \infty$ the integrand $f(k)$ increases as k^2/S. The large-k (short-distance) behaviour is associated with hard-sphere ordering. This ordering is not described correctly by the present field theory, because of the local-density approximation for F_h in equation (9). The divergency of $\mathcal{G}_0$ is an artefact of this approximation. We can regularize the integral in (40) by introducing a cutoff $\Lambda \approx \pi$. In our theory the natural cutoff corresponds to the shortest possible period of the oscillatory decay of charge correlations, 2σ, and we choose $\Lambda = \pi$ in σ^{-1} units. Dependence on Λ in the field theory indicates dependence on the form of the reference-system free energy. Note that $\mathcal{G}_0 = G^0_{\phi\phi}(0)$. Alternatively, the integral (40) can be regularized by assuming $\mathcal{G}_0 = G^0_{\phi\phi}(\sigma)$.

The properties of the cutoff-regularized integral depend crucially on S. For

$$S = S_0 \approx 2.58 \tag{42}$$

the $f(k)$ has an inflection point for $k \approx 3.32$. For $S > S_0$ the $f(k)$ increases monotonically, and for $S < S_0$ a maximum and a minimum appear for $k_{\max} < \pi$ and for $k_{\min} > \pi$, respectively (see figure 3). For $S \to S_\lambda$ the maximum of $f(k)$ moves to $k = k_b$ and increases to infinity, and $f(k)$ can be written in the form

$$f_0(k) \simeq_{S\to S_\lambda} \frac{k^2}{S - S_\lambda + v_2(k - k_b)^2}. \tag{43}$$

The integral

$$\mathcal{G}_0 = \frac{T^*}{2\pi^2}\int_0^\Lambda \mathrm{d}k\, f_0(k) \tag{44}$$

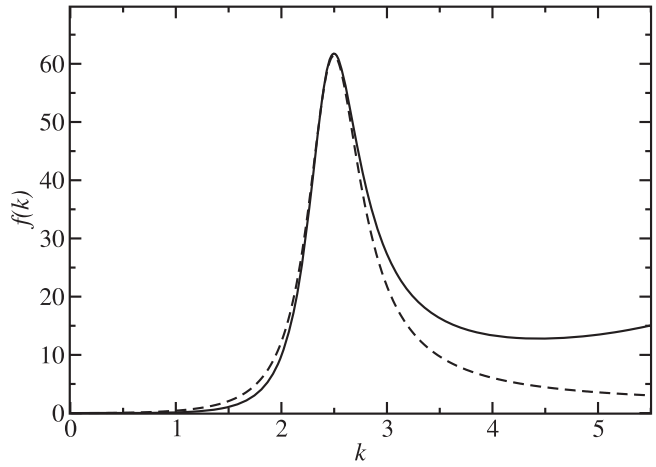

Figure 3. The integrand $f(k)$ in equation (40) (solid line) and the approximate form (43) (dashed line) for $S = 1.712$ ($S - S_\lambda = 0.1$).

can be evaluated analytically. The cutoff-regularized integral (40) is analysed in more detail in appendix B, where we find the asymptotic results

$$\mathcal{G}_0(S) \simeq \begin{cases} \dfrac{T^*\Lambda^3}{6\pi^2 S} = \dfrac{\rho_0^*\Lambda^3}{6\pi^2} & \text{if } S \to \infty \\ \dfrac{T^* k_b^2}{2\pi\sqrt{v_2(S - S_\lambda)}} + \dfrac{T^*\Lambda}{2\pi^2 v_2} + \mathrm{O}(\log\Lambda) & \text{if } S - S_\lambda \ll v_2 k_b^2. \end{cases} \tag{45}$$

Note that for $S - S_\lambda \ll v_2 k_b^2$ the first contribution to $\mathcal{G}_0(S)$ is cutoff independent. For $\Lambda \approx \pi$ the cutoff-dependent contribution is negligible when compared to the first term. Since the main contribution to $\mathcal{G}_0(S)$ is independent of Λ, the precise form of the hard-sphere reference-system free energy is not important, and our approach can give quantitatively correct results beyond MF. This is because for $k \approx k_b$ the ordering of charges (nearest neighbours oppositely charged) takes place as a result of the tendency for minimizing the electrostatic energy. For $S > S_0$ the wavenumbers $k \approx \Lambda$ yield the main contribution to $\mathcal{G}_0(S)$. No other wavelength is distinguished, since $f(k)$ increases monotonically. Strong Λ-dependence of $\mathcal{G}_0(S)$ indicates that the reference system plays an important role and a better approximation for F_h is necessary in order to obtain accurate results. In such a case microscopic theories are superior to our approach. Our first conclusion is that quantitatively correct results in this field theory can in principle be obtained for $S - S_\lambda \ll v_2 k_b^2$, and cannot be obtained for $S > S_0$. Recall that in practice we consider the truncated expansion in equation (28). The accuracy of the results depends on the truncation, but can be systematically improved by including higher-order terms in equation (28).

Let us consider the criterion (39) in the cutoff-regularized theory. In order to evaluate $\tilde{b}(k)$ we assume $\Lambda = \pi$. For $k \to 0$ we find from equations (45) and (22) the asymptotic behaviour

$$\tilde{b}(k) \simeq_{k\to 0} Bk^2$$

with

$$B \approx \begin{cases} \dfrac{\mathcal{A}_4 \rho_0^{*2} S}{48} & \text{if } S \to \infty, \quad \Lambda = \pi \\ \dfrac{\mathcal{A}_4 \rho_0^{*2} S^2 k_b^2}{16\pi^2\sqrt{v_2(S - S_\lambda)}} & \text{if } S - S_\lambda \ll v_2 k_b^2, \end{cases}$$

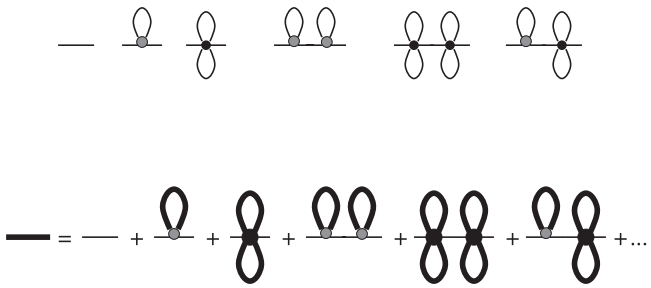

Figure 4. Top: a few Feynman diagrams contributing to $G_{\phi\phi}$ in the one-loop approximation (46). The symbols are the same as in figure 2. Bottom: the graphical representation of the self-consistent equation for $G^{\mathrm{H}}_{\phi\phi}$, represented by the thick line. The thin line represents $G^{0}_{\phi\phi}$.

where $\mathcal{A}_4$ is given in appendix A. The correction term is negligible for $k \ll 1/\sqrt{B}$. For any given thermodynamic state $\tilde{G}^{0}_{\phi\phi}(k)$ can be arbitrarily close to the exact result $\tilde{G}_{\phi\phi}(k)$ for sufficiently small k. For this reason for $k \to 0$ our MF result is identical to the exact expression, as observed in section 2.2.

For $k \neq 0$ the MF result departs from the exact form of the correlation function. For a given thermodynamic state the maximum of the correction term is assumed for $k = k_b$, and the corresponding form of $\tilde{b}(k_b)$ is

$$\tilde{b}(k_b) \simeq \begin{cases} \dfrac{\pi}{12}\mathcal{A}_4\rho_0^{*2} & \text{if } S \to \infty, \quad \Lambda = \pi \\ \dfrac{\mathcal{A}_4\rho_0^{*2}S^2k_b^2}{4\pi\sqrt{v_2(S-S_\lambda)^3}} & \text{if } S - S_\lambda \ll v_2k_b^2, \end{cases}$$

In the case of large S the correction term depends only on ρ_0^*, and we find that $\tilde{b}(k_b) < 0.975$. The MF result is not quantitatively correct, but at least the correction term is not large. For $S \to S_\lambda$, however, the correction term diverges as $(S - S_\lambda)^{-3/2}$ with a prefactor that is larger than unity. For $S - S_\lambda \ll 1$ the MF result is qualitatively wrong, and the terms beyond the first one must be included in the perturbation expansion discussed at the beginning of this section. This will be done within the Brazovskii theory in the next section.

The condition (39) is valid in other physical systems with the OP denoted by ϕ, the OP correlation function denoted by $G_{\phi\phi}$, and with $\mathcal{A}_4$ denoting the four-point vertex function (inverse correlation function) $\delta^4\Omega^{\mathrm{MF}}/\delta\phi(\mathbf{x})^4$, calculated at one point in the local-density approximation. In systems where any kind of periodic ordering leading to some sort of crystalline structures occurs, the MF approximation for the correlation function, $G^{0}_{\phi\phi}(x)$, can be valid sufficiently far from the MF line of instability (λ-line), provided that the four-point vertex function (inverse correlation function) for nearest neighbours is sufficiently small, and both $G^{0}_{\phi\phi}(x)$ and $G^{0}_{\phi\phi}(\sigma)$ are small too.

4. Correlation functions in the one-loop approximation

4.1. Perturbation expansion

In this section the perturbation theory [34, 35] outlined in section 3 is considered to an infinite order, and $\tilde{G}_{\phi\phi}$ is calculated in the effectively one-loop approximation. In this approximation the Feynman diagrams shown in figure 4 (top) are included, and $\tilde{G}_{\phi\phi}$ has a form of the

geometric series

$$\tilde{G}_{\phi\phi} \approx \tilde{G}^0_{\phi\phi} \sum_{n=0} (q\tilde{G}^0_{\phi\phi}(k))^n, \tag{46}$$

where in the ϕ^6 theory

$$q = -\left(\frac{\mathcal{A}_4\mathcal{G}_0}{2} + \frac{\mathcal{A}_6\mathcal{G}_0^2}{8}\right). \tag{47}$$

The inverse function in this approximation is given by

$$\tilde{C}_{\phi\phi}(k) \approx \tilde{C}^0_{\phi\phi}(k) - q. \tag{48}$$

The approximate expression (48) for the inverse charge-density correlation function can be rewritten in the form

$$\tilde{C}_{\phi\phi}(k) = \left(S^{\mathrm{H}} + \frac{4\pi\cos k}{k^2}\right)\beta^*, \tag{49}$$

which is the same as the form of $\tilde{C}^0_{\phi\phi}(k)$ (see equations (19) and (11)), except that $S = T^*/\rho_0^*$ is replaced by the renormalized quantity

$$S^{\mathrm{H}} = S - qT^*. \tag{50}$$

According to the results of section 3, the form of q defined in equation (47) depends qualitatively on S.

For $S > S_0$ we have (see (45)) in the ϕ^6 theory (28)

$$q = -\left[\frac{\mathcal{A}_4\rho_0^*}{2}\frac{\Lambda^3}{6\pi^2} + \frac{\mathcal{A}_6\rho_0^{*2}}{8}\left(\frac{\Lambda^3}{6\pi^2}\right)^2\right]. \tag{51}$$

From (49)–(51) and from the result of [15] we obtain the Kirkwood line, $S^{\mathrm{H}} = 11.8$, given by the explicit expression

$$T^*(\rho_0^*) = \frac{11.8\rho_0^*}{1 - q\rho_0^*}. \tag{52}$$

Because of the strong cutoff dependence, results of our theory are inaccurate for $S > S_0$, as discussed in section 3. Since the accuracy of the results is limited by the local-density approximation for the reference system, we shall not try to improve the perturbation expansion about the MF result for $S > S_0$.

For $S < S_0$ the results are independent of the precise form of the reference-system free energy, and our theory is reliable in this part of the phase diagram. The accuracy of our result is limited only by the truncation of the expansion in ϕ^2 in equation (28), and by the accuracy of the perturbation expansion. We can improve the accuracy of the one-loop approximation by considering the self-consistent theory. In equation (48), q is the functional of $\tilde{G}^0_{\phi\phi}(k)$ (see equation (38) for $\mathcal{G}_0$). In the self-consistent, effectively one-loop Hartree approximation [29], q is the functional of the same form, but of $\tilde{G}^{\mathrm{H}}_{\phi\phi}(k) = 1/\tilde{C}^{\mathrm{H}}_{\phi\phi}(k)$, which is the result of the whole resummation in equation (46). The inverse correlation function in the self-consistent approximation assumes the form (see (49) (50) and (19)) [25, 29, 30]

$$\tilde{C}^{\mathrm{H}}_{\phi\phi}(k) = r_0 + v_2(k - k_b)^2\beta^*, \tag{53}$$

where

$$r_0 = \beta^*(S - S_\lambda) - q(r_0), \tag{54}$$

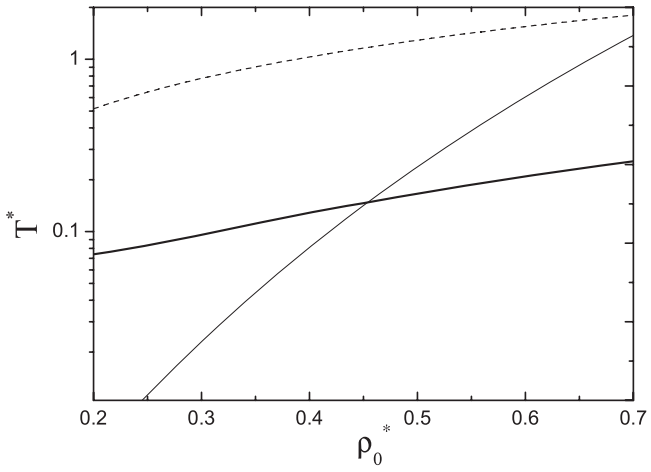

Figure 5. The thin solid line represents $T^* = v_2 k_b^4/\mathcal{A}_4^2$, and the dashed line is $S = S_0 \approx 2.58$. For $T^* \ll v_2 k_b^4/\mathcal{A}_4^2$ and $S < S_0$ the results of the self-consistent one-loop approximation are correct. In the rest of the phase diagram either the remaining Feynman diagrams (including the one shown in figure 2(b)) have to be included, or the approximate form of $\mathcal{G}(r_0)$, equation (55), is not valid. The thick solid line represents the phase transition found in [12].

and where in the self-consistent approximation $q(r_0)$ is given in equation (47), but with $\mathcal{G}_0$ replaced by

$$\mathcal{G}(r_0) = \frac{T^*}{2\pi^2}\int \mathrm{d}k\, k^2 \tilde{G}^{\mathrm{H}}_{\phi\phi}(k) = \frac{k_b^2\sqrt{T}^*}{2\pi\sqrt{v_2 r_0}}. \tag{55}$$

In the above the result of appendix B (with $\beta^*(S - S_\lambda)$ replaced by r_0) is used. The self-consistent solution of equations (54) and (47) with $\mathcal{G}_0$ replaced by $\mathcal{G}(r_0)$, equation (55), can be found analytically. The explicit expression for r_0 is given in appendix C.

For $S < S_0$ our Brazovskii-type approximation relies on two important assumptions, and therefore it is valid only in a limited region of the phase diagram. The first assumption, discussed in section 3 and in appendix B in the context of validity of equation (55), is $r_0 \ll \beta^* v_2 k_b^2$. The second assumption is that the contributions to $\tilde{G}_{\phi\phi}(k)$ associated with the two-loop diagrams (including the diagram shown in figure 2(b)) are negligible compared to the one-loop diagrams. As shown by Brazovskii [29], the two-loop (figure 2(b)) and higher-order diagrams can be neglected if $\mathcal{A}_4\sqrt{\beta^* v_2} \ll r_0$. From the two above conditions we obtain the region in the phase diagram,

$$T^* \ll \frac{v_2 k_b^4}{\mathcal{A}_4^2} \qquad \text{and} \qquad S < S_0 \approx 2.58, \tag{56}$$

where equations (53) and (55) give accurate results in the field theory corresponding to the Hamiltonian (28). The line $T^* = v_2 k_b^4/\mathcal{A}_4^2$ is shown in figure 5 together with the coexistence line obtained in [12]. Note that the assumptions of our theory are satisfied near the phase coexistence for the high densities $\rho_0^* > 0.5$.

The charge-density correlation function in real space can be obtained by following the pole analysis of [15], just by substituting S^{H} for S. For $S \gg S_0$ the S^{H} is given in equations (50) and (51), and for $S \to S_\lambda$ the renormalized quantity (50) takes the form

$$S^{\mathrm{H}} = T^* r_0 + S_\lambda. \tag{57}$$

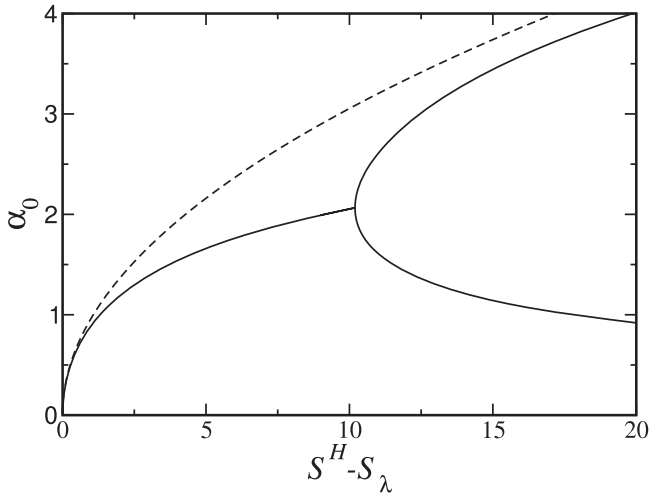

Figure 6. The inverse decay length α_0 of the charge-density correlation function, as a function of $S^{\mathrm{H}} - S_\lambda$. The line $\alpha_0(S^{\mathrm{H}} - S_\lambda)$ splits into two branches representing a_1 and a_2 at the Kirkwood line (52). The dashed line is the inverse decay length obtained from the approximate form of $\tilde{C}_{\phi\phi}(k)$ (equation (53)). For the relation of $S^{\mathrm{H}} - S_\lambda$ to thermodynamic variables see the text.

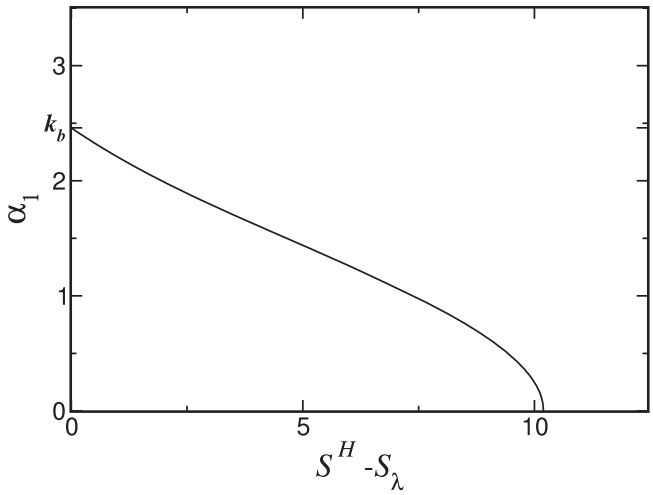

Figure 7. $\alpha_1 = 2\pi/\lambda$, where λ is the period of damped oscillations of $G_{\phi\phi}(x)$, as a function of $S^{\mathrm{H}} - S_\lambda$. For the relation of $S^{\mathrm{H}} - S_\lambda$ to thermodynamic variables see the text.

In the former case the one-loop approximation is used, and in the latter case the self-consistent one-loop approximation is used. The inverse lengths α_0 and α_1 are shown in figures 6 and 7 as functions of $S^{\mathrm{H}} - S_\lambda$, where the numerical results obtained in [15] are used. The relation between $S^{\mathrm{H}} - S_\lambda$ and thermodynamic quantities is not trivial, and in the one-loop approximation is based on equation (50). Explicit expression for $S^{\mathrm{H}} - S_\lambda$, based on the above results, can be given in the limiting cases, $S \gg S_0$, or $S - S_\lambda \ll k_b^2$. The condition equivalent to $S \gg S_0$ has the form $S^{\mathrm{H}} - S_\lambda \gg S_0 - S_\lambda - qT^* = S_0(1 - q\rho_0^*) - S_\lambda > 5$ (equations (50) and (51) were used), and in this regime $S^{\mathrm{H}} - S_\lambda \approx S - S_\lambda - T^*q$, where q is given in equation (51).

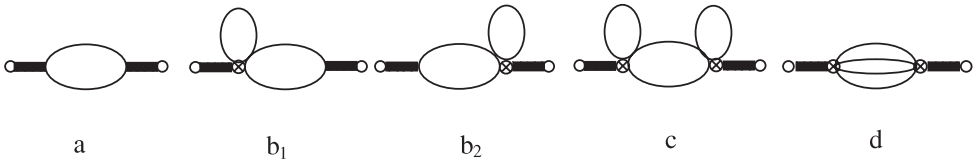

Figure 8. Feynman diagrams contributing to the approximate form of $G_{\eta\eta}(\mathbf{x}_1, \mathbf{x}_2)$ given in equation (58), for $\mathbf{x}_1 \neq \mathbf{x}_2$. Open circles represent external points $\mathbf{x}_1$ and $\mathbf{x}_2$. Lines connecting points $\mathbf{x}$ and $\mathbf{x}'$ represent $G^{\mathrm{H}}_{\phi\phi}(\mathbf{x} - \mathbf{x}')$. The black box represents $G^{0}_{\eta\eta} = 1/\gamma_{0,2}$. The vertex from which the box and the two thin lines emanate represents $-\gamma_{2,1}$ and the circle with a cross inside represents $\Gamma^{0}_{4,1}$ (for the relation between the above coefficients and a_i see appendix A, equation (A.1)). Symmetry factors are calculated according to standard rules [34, 35]. Diagram (a) represents the first, diagrams (b) represent the second, and diagrams (c) and (d) represent the third and the fourth contributions to equation (58) respectively.

When $S < S_0$ and $S^{\mathrm{H}} - S_\lambda \ll k_b^2$, then $S^{\mathrm{H}} - S_\lambda \approx T^* r_0(\rho_0^*, T^*)$, where $r_0(\rho_0^*, T^*)$ is the self-consistent solution of equations (48) and (55). For the explicit form of r_0 see appendix C. Note that the range of correlations diverges ($\alpha_0 = 0$) for $T^* r_0 = 0$ (see figure 6). From the explicit result for r_0 (appendix C) it follows that, when $T^* > 0$, then $r_0 > 0$ as well. The range of charge-density correlations is thus finite, in agreement with the results of the MSA and related approximations [3, 5], as well as with simulations.

Let us focus on the number-density correlation function in the weighted-field approximation. In equation (30) $G_{\eta\eta}$ is given in terms of higher-order correlation functions for the field ϕ. In the one-loop self-consistent approximation, equation (30) assumes the form

$$G^{\mathrm{H}}_{\eta\eta}(\mathbf{x}, \mathbf{x}') = G^{0}_{\eta\eta}\delta(\mathbf{x}, \mathbf{x}') + (2a_1^2 + 12a_1a_2\mathcal{G}(r_0) + 18a_2^2\mathcal{G}(r_0)^2)G^{\mathrm{H}}_{\phi\phi}(\mathbf{x}, \mathbf{x}')^2 + 3!a_2^2 G^{\mathrm{H}}_{\phi\phi}(\mathbf{x}, \mathbf{x}')^4, \tag{58}$$

and this is represented graphically in figure 8. The numerical factors in equation (58) are obtained in a standard way [34, 35].

4.2. Correlation functions at the coexistence with the ionic crystal

The transition between the liquid and ionic crystal was found in [12] in an approach consistent with the self-consistent one-loop approximation outlined in section 4.2. Note that in the one-loop approximation $T^*\tilde{C}_{\phi\phi}(k)$ depends on the thermodynamic state through a single variable S^{H}. Since the phase coexistence takes place for $r_0 \ll \beta^* v_2 k_b^2$, $\beta^* G^{\mathrm{H}}_{\phi\phi}$ depends on the thermodynamic state only through $S^{\mathrm{H}} = T^* r_0 + S_\lambda$ (equation (50)). From the explicit result for r_0 (appendix C), and the result for the coexistence line $T^*(\rho_0^*)$ obtained in [12], we obtain $r_0(\rho_0^*)$ shown in figure 9, and in turn we find $T^* r_0 \approx 0.2$ for $0.25 < \rho_0^* < 0.8$. Thus, along the phase coexistence line the inverse lengths are nearly independent of density, and their numerical values are found to be $\alpha_0 \approx 0.97$ and $\alpha_1 \approx 2.26$ (see figures 6 and 7). The approximate results for the amplitude and the phase are [15] $-\mathcal{A}_{\phi\phi} \approx 0.23 S^{\mathrm{H}}/\sqrt{S^{\mathrm{H}} - S_\lambda} \approx 0.96$ and $\theta \approx 0.88\sqrt{S^{\mathrm{H}} - S_\lambda} \approx 3.81$, respectively. The correlation functions along the phase coexistence are shown in figures 10 and 11.

The inverse lengths α_0 and α_1 depend on the thermodynamic state through a single variable also in the MSA and related approximations [5], and $x_{\mathrm{D}} = \kappa_{\mathrm{D}}\sigma = \sqrt{4\pi/S}$ is usually chosen. Note that in our theory S^{H} reduces to S in MF; thus, the parameter $\sqrt{4\pi/S^{\mathrm{H}}}$ reduces to x_{D}. At the transition we find $\sqrt{4\pi/S^{\mathrm{H}}} \approx 2.25$. The characteristic inverse lengths in the GMSA for $x_{\mathrm{D}} \approx 2.25$ can be read off from figure 4 of [5], and they are $\alpha_0 \approx 1.5$ and $\alpha_1 \approx 2.1$. More precise values are given in [5] for $x_{\mathrm{D}} = 4$, where $\alpha_0 = 1.32$ and $\alpha_1 = 2.89$, and for $x_{\mathrm{D}} = 1.5$,

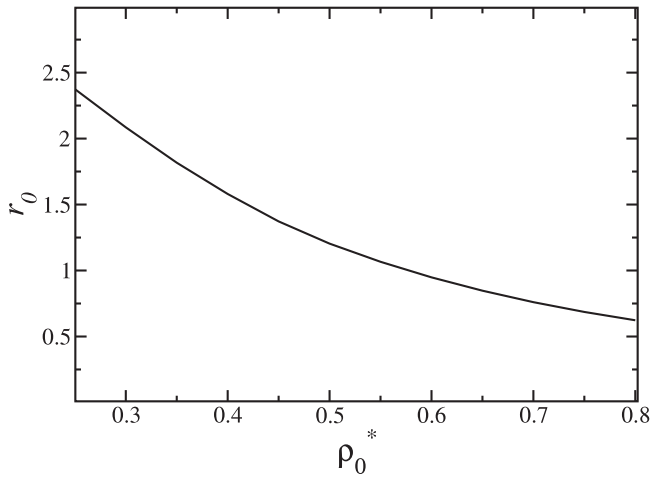

Figure 9. $r_0(\rho_0^*)$ along the coexistence line $T^*(\rho_0^*)$ between liquid and the charge-ordered phase in the ϕ^6-theory.

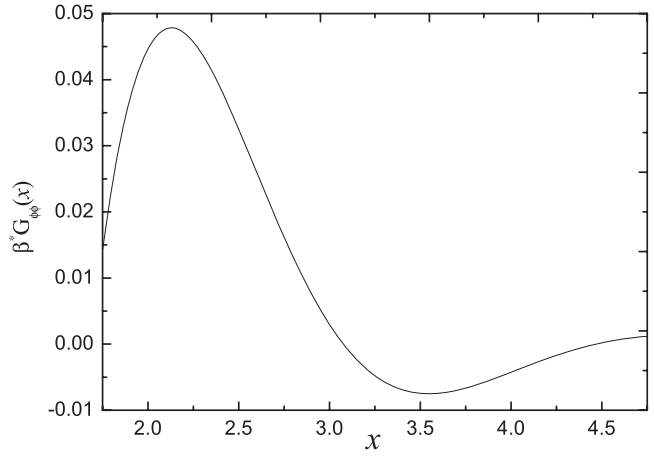

Figure 10. Charge-density correlation function $\beta^* G^{\mathrm{H}}_{\phi\phi}(x)$ in the liquid phase for $S^{\mathrm{H}} \approx 1.8$ corresponding to the coexistence with the charge-ordered phase. $\beta^* G^{\mathrm{H}}_{\phi\phi}(x)$ is dimensionless and x is in σ units.

where $\alpha_0 = 2.15$ and $\alpha_1 = 1.22$. Rather good agreement between the two theories is obtained, although in our theory the decay length is larger than in the GMSA. Similar fair agreement is obtained for the amplitude and the phase shift.

Note that the form of $\beta^* G^{\mathrm{H}}_{\phi\phi}(x)$ is the same along the phase coexistence, for a large range of density. This result is consistent with the structure of the ionic crystal coexisting with the liquid, where the nn distance is also independent of density on the same level of approximation. This result reflects the fact that the tendency for ordering in periodic structure follows directly from the form of the Coulomb potential, and not from the close packing of hard spheres.

The number-density correlation function is shown in figure 11. In our theory the contribution to the correlation functions associated with hard-sphere ordering is neglected. The number-density correlation function shown in figure 11 results from the coupling between the number-density and the charge-density fluctuations, and is induced by the charge ordering,

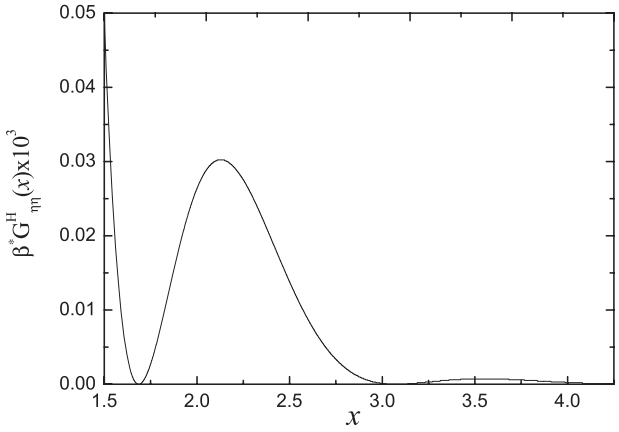

Figure 11. Charge-density fluctuation contribution to the number-density correlation function $\beta^* G^{\mathrm{H}}_{\eta\eta}(x)$ (equation (58)) in the liquid phase at the coexistence with the charge-ordered phase for $\rho_0^* = 0.7$. In our theory the hard-sphere contribution has the form $G^0_{\eta\eta}\delta(x)$. In a more accurate theory the hard-sphere contribution should be added to the above result. Note that $\beta^* G^{\mathrm{H}}_{\eta\eta}(x)$ is three orders of magnitude smaller than the charge-density correlation function.

which in turn follows from the form of the interaction potential. The exact form of the number-density correlation function should contain the entropic contribution due to the hard-sphere ordering, in addition to the interaction-induced contribution shown in figure 11.

5. Summary

In this work the fluctuation contributions to the charge-density and the number-density correlation functions in the RPM are calculated within the Brazovskii-type theory. In MF the amplitude and the correlation length both diverge when the λ-line is approached. At the low-temperature side of the λ-line an instantaneous order occurs in the majority of the individual microscopic states, i.e. clusters with oppositely charged nns dominate over randomly distributed ions. Averaging over microscopic states with somewhat different order leads to a homogenization of the structure down to the fluctuation-induced first-order transition to the ionic crystal. Our purpose here was a verification if the instantaneous order found on the low-T side of the λ-line leaves some traces in the correlation functions. Our results show that the correlation length and the amplitude of $G_{\phi\phi}(x)$, both divergent in MF at the λ-line, show no indication of the MF singularity when the fluctuation contribution is included. Both quantities are of order of unity in the whole stability region of the fluid phase. It is worth noting that a similar breakdown of the MF approximation is expected in other systems exhibiting fluctuation-induced first-order phase transitions. This breakdown is expected in this part of the phase diagram, where the simple criterion (39) is not satisfied.

We should stress that the characteristic lengths in equation (4) are independent of density along the phase coexistence, even though the crystallization occurs for a range of densities that is much larger than in simple uncharged systems (see figure 1 and references [12, 13]). On the other hand, the amplitude of the correlation function increases with density along the phase coexistence. This observation indicates that when the density is decreased, vacancies appear in the neighbourhood of each ion, whereas the most probable nn distance, π/α_1, and the range of order, α_0^{-1}, stay unchanged.

Finally let us summarize the approximations that we make and the accuracy of our results. We start with the probability measure (6), where the local-density approximation is assumed

for the hard-sphere reference system. Because of that approximation the effects associated with hard-spheres ordering cannot be accurately described. As discussed in detail in section 3, the dominant contribution to the charge-density correlation function is independent of the form of the reference-system free energy in the relevant part of the phase diagram (figure 5). Thus, the local-density approximation is justified when the charge-density correlation function near the coexistence with the crystal is studied. However, this assumption influences our results for the number-density correlation function (see figure 11). Next we assume the WF approximation (section 2.3) and limit ourselves to the ϕ^6 effective Hamiltonian (28) given in terms of the OP describing fluctuations of the charge density ϕ. We limit ourselves to the ϕ^6 theory, since the phase coexistence was determined in this approximation. The accuracy of the theory can be systematically improved by including subsequent terms $\propto \phi^{2n}$ in equation (28). This point was already discussed in [12], where the phase transition was found in the ϕ^4 and in the ϕ^6 theories. The results of the ϕ^6 theory agree better with simulations [13]. The distance between the crystallization lines obtained in the two approximations is much smaller than the distance between either one of these lines and the λ-line. We expect that the results of the ϕ^6 theory for the correlation functions are correct on the semiquantitative level as well. Based on the Hamiltonian (28) the charge-density correlation function is calculated using the one-loop self-consistent Hartree approximation. The contributions to the charge-density correlation function beyond that approximation can be neglected in the region of the phase diagram where conditions (56) are satisfied, as discussed in more detail in section 4.

Acknowledgment

This work was supported by the Polish Ministry of Science and Education through the research project 1 P03B 033 26.

Appendix A. Coefficients $\mathcal{A}_4$, $\mathcal{A}_6$, a_1 and a_2 in the WF approximation

$$\mathcal{A}_4 = \gamma_{4,0} - 3\frac{(-\gamma_{2,1})^2}{\gamma_{0,2}},$$

$$\mathcal{A}_6 = \gamma_{6,0} - 15\frac{(-\gamma_{2,1})(-\gamma_{4,1})}{\gamma_{0,2}} - 15\frac{(-\gamma_{2,1})^3(-\gamma_{0,3})}{\gamma_{0,2}^3} - 45\frac{(-\gamma_{2,2})(-\gamma_{2,1})^2}{\gamma_{0,2}^2},$$

where

$$\gamma_{2m,n} = \left.\frac{\partial^{2m+n} f_h(\phi,\rho)}{\partial\phi^{2m}\partial\rho^n}\right|_{\phi=0,\rho=\rho_0^*}.$$

In the CS approximation they assume the explicit forms

$$\mathcal{A}_4 = -\frac{1-20s+10s^2-4s^3+s^4}{\rho_0^{*3}(1+4s+4s^2-4s^3+s^4)}$$

and

$$\mathcal{A}_6 = \frac{3W(s)}{\rho_0^{*5}(1+4s+4s^2-4s^3+s^4)^5},$$

with $s = \pi\rho_0^*/6$ and

$$W(s) = 3 - 84s + 360s^2 + 2644s^3 + 1701s^4 - 8736s^5 + 11\,240s^6 - 8304s^7 + 3861s^8 - 1164s^9 + 240s^{10} - 36s^{11} + 3s^{12}.$$

The coefficients a_1 and a_2 in equation (29) are

$$a_1 = -\frac{\gamma_{2,1}}{2!\gamma_{0,2}}, \qquad \frac{a_2}{2} = -\frac{\Gamma^0_{4,1}}{4!\gamma_{0,2}}, \tag{A.1}$$

where

$$\Gamma^0_{4,1} = \gamma_{4,1} - \frac{6(-\gamma_{2,2})(-\gamma_{2,1})}{\gamma_{0,2}} - \frac{3(-\gamma_{3,0})(-\gamma_{2,1})^2}{\gamma^2_{0,2}}. \tag{A.2}$$

Appendix B. Analysis of $\mathcal{G}_0 = T^* g(S)$

Let us first consider $S \gg S_0$. Note that $f(k)$ can be written in the form

$$f(k) = \frac{k^2}{S} - \frac{4\pi}{S^2}\frac{\cos k}{1 + \frac{4\pi\cos k}{Sk^2}}. \tag{B.1}$$

For $\Lambda \approx \pi$ and for $S \gg S_0$ the second term in (B.1) gives a negligible contribution to $\mathcal{G}_0$, and we obtain

$$\mathcal{G}_0(S) = \frac{T^*}{2\pi^2}\int_0^\Lambda \mathrm{d}k\, f(k) = \frac{T^*\Lambda^3}{6\pi^2 S} + \mathrm{O}(S^{-2}).$$

Let us focus on $S_\lambda < S < S_0$, and write $f(k)$ in the form

$$f(k) = f_0(k) + \Delta f(k),$$

where $f_0(k)$ is given in equation (43). When $(f(\Lambda) - f_0(\Lambda))/f_0(k_b) \ll 1$, which is the case for $\Lambda \approx \pi$, because $(f(\pi) - f_0(\pi))/f_0(k_b) < 0.15$, then $\Delta f(k)$ yields a negligible contribution to $\mathcal{G}_0$. The explicit form of the integral (44) is

$$\mathcal{G}_0(S) = \frac{T^* k_b^2}{2\pi^2\sqrt{v_2(\Delta S)}}\left(1 - \frac{\Delta S}{v_2 k_b^2}\right)\left[\arctan\left(\sqrt{\frac{v_2}{\Delta S}}(\Lambda - k_b)\right) + \arctan\left(k_b\sqrt{\frac{v_2}{\Delta S}}\right)\right] + \frac{T^*\Lambda}{2\pi^2 v_2} + \frac{T^* k_b}{2\pi^2 v_2}\log\left[\frac{\Delta S + (\Lambda - k_b)^2 v_2}{\Delta S + k_b^2 v_2}\right],$$

where $\Delta S = S - S_\lambda$. For $\Delta S \ll v_2 k_b^2$ we obtain

$$\mathcal{G}_0(S) \simeq \frac{T^* k_b^2}{2\pi\sqrt{v_2(\Delta S)}} + \frac{T^*\Lambda}{2\pi^2 v_2} + \mathrm{O}(\log\Lambda).$$

Appendix C. Explicit expression for r_0

By solving equations (54) (taking into account (47), (48) and (55)) we obtain in the case of $\tau_0 = 1/(\beta^*\rho_0^*) + \tilde{V}(k_b) < 0$ the explicit expression for r_0,

$$r_0 = \tfrac{1}{2}\left[\sqrt{u + v - p/3} + \sqrt{2(h - (u+v)/2 - p/3)} + \tau_0\right],$$

where the following notations are introduced:

$$u = \left(-b_2 + \sqrt{b_1^3 + b_2^2}\right)^{1/3}, \qquad v = \left(-b_2 - \sqrt{b_1^3 + b_2^2}\right)^{1/3},$$

$$b_1 = -\frac{1}{3}\left(\frac{p^2}{12} + 8a^2 T^* \mathcal{A}_4^2 \tau_0\right), \qquad b_2 = \left(-\frac{p}{6}\right)^3 + \frac{4}{3}pa^2 T^* \mathcal{A}_4^2 \tau_0 - \frac{q^*}{2}$$

$$h = [((u+v)/2 + p/3)^2 + 3(u-v)^2/4]^{1/2}$$

$$p = -(\tau_0^2 + 2a^2 T^* \mathcal{A}_6), \qquad q^* = a^4 T^{*2} \mathcal{A}_4^4$$

$$a = k_b^2/(4\pi\sqrt{v_2}).$$

References

[1] Debye P and Hückel E 1923 *Z. Phys.* **24** 185
[2] Fisher M E 1994 *J. Stat. Phys.* **75** 1
[3] Stell G 1995 *J. Stat. Phys.* **78** 197
[4] Stillinger F H and Lovett R 1968 *J. Chem. Phys.* **48** 3858
[5] Leote de Carvalho R J F and Evans R 1994 *Mol. Phys.* **83** 619
[6] Leote de Carvalho R J F and Evans R 1995 *J. Phys.: Condens. Matter* **7** 575
[7] Evans R, Leote de Carvalho R J F, Henderson J R and Hoyle D C 1994 *J. Chem. Phys.* **100** 591
[8] Leote de Carvalho R J F, Evans R and Rosenfeld Y 1999 *Phys. Rev.* E **59** 1435
[9] Evans R and Leote de Carvalho R J F 1996 *Chemical Applications of Density-Functional Theory* (*ACS Symposium Series* vol 629) ed B B Laird, R B Ross and T Ziegler (Washington DC: American Chemical Society) chapter 12
[10] Barrat J-L 1987 *J. Phys. C: Solid State Phys.* **20** 1031
[11] Ciach A and Stell G 2000 *J. Mol. Liq.* **87** 253
[12] Ciach A and Patsahan O 2006 *Phys. Rev.* E **74** 021508
[13] Vega C, Abascal J L F, McBride C and Bresme F 2003 *J. Chem. Phys.* **119** 964
[14] Outhwaite C 1975 *Statistical Mechanics. A Specialist Periodic Report* vol 2, ed K Singer (London: The Chemical Society) p 188
[15] Ciach A, Góźdź W T and Evans R 2003 *J. Chem. Phys.* **118** 3702
[16] Patsahan O and Mryglod I 2004 *Condens. Matter Phys.* **7** 755
[17] Panagiotopoulos A Z and Kumar S K 1999 *Phys. Rev. Lett.* **83** 2981
[18] Diehl A and Panagiotopoulos A Z 2003 *J. Chem. Phys.* **118** 4993
[19] Dickman R and Stell G 1999 *Simulation and Theory of Electrostatic Interactions in Solution* (*AIP Conference Proceedings* vol 492) ed L Pratt and G Hummer (Melville, NY: AIP)
[20] Ciach A and Stell G 2001 *J. Chem. Phys.* **114** 3617
[21] Kobelev V, Kolomeisky A B and Fisher M E 2002 *J. Chem. Phys.* **117** 8897
[22] Brognara A, Parola A and Reatto L 2002 *Phys. Rev.* E **65** 66113
[23] Artyomov M N, Kobelev V and Kolomeisky A B 2003 *J. Chem. Phys.* **118** 6394
[24] Ciach A and Stell G 2003 *Phys. Rev. Lett.* **91** 060601
[25] Ciach A and Stell G 2005 *Int.J. Mod. Phys.* B **21** 3309
[26] Panagiotopoulos A Z and Fisher M E 2002 *Phys. Rev. Lett.* **88** 45701
[27] Weis J-J, Levesque D and Caillol J-M 1998 *J. Chem. Phys.* **109** 7486
[28] Spohr E, Hribar B and Vlachy V 2002 *J. Phys. Chem.* B **106** 2343
[29] Brazovskii S A 1975 *Sov. Phys.—JETP* **41** 8
[30] Ciach A 2004 *Phys. Rev.* E **70** 046103
[31] Ciach A, Góźdź W T and Stell G 2006 *J. Phys.: Condens. Matter* **18** 1629
[32] Ciach A and Stell G 2001 *J. Chem. Phys.* **114** 382
[33] Ciach A 2006 *Phys. Rev.* E **73** 066110
[34] Amit D J 1984 *Field Theory, the Renormalization Group and Critical Phenomena* (Singapore: World Scientific)
[35] Zinn-Justin J 1989 *Quantum Field Theory and Critical Phenomena* (Oxford: Clarendon)